33rd Annual International Conference of the IEEE EMBS
Boston, Massachusetts USA, August 30 - September 3, 2011

Coupling Biotic and Abiotic Metrics to Create a Testbed for Predicting Neural Electrode Performance

Abhishek Prasad, *Member IEEE*, Viswanath Sankar, *Member IEEE*, Aubrey T. Dyer, Eric Knott, Qing-Shan Xue, Toshikazu Nishida, *Senior Member IEEE*, John R. Reynolds, Gerry Shaw, Wolfgang Streit, and Justin C. Sanchez, *Member IEEE*

***Abstract*— In this work, we develop an experimental testbed that couples biotic and abiotic metrics for studying, quantifying and predicting the effects of chronic electrode implantation on neural electrode performance. The rationale is based on the observation that long-term functionality is the outcome of the interactions between the dynamics of the neuronal environment and the properties of the electrode itself. By combining and analyzing the substantially richer information available in the spatiotemporal dynamics of neurons with biotic and abiotic metrics such as biochemical markers, histochemistry, SEM imaging, and electrochemistry, we seek to quantitatively improve our understanding of the functional modifications underlying the long-term responses of electrode implants. The goal is to ultimately enable the design of future reliable interfaces. In our preliminary analysis using this biotic-abiotic approach of an electrode 18 days post-implant, we observed both structural and histochemical responses related to chronic electrode implantation. These were coupled to daily functional changes in electrode performance. Interestingly, these changes were not correlated with markers of brain injury at the time of electrode explantation. Future work using this multidisciplinary approach is directed to providing a detailed perspective into long-term microelectrode performance.**

I. Introduction

THE development of invasive, rehabilitative neuroprosthetics for humans requires reliable neural probes that are capable of recording large ensembles of neurons for long periods of time. As a result, research has focused on the cascade of events that follow chronic implantation of microelectrodes and the temporal degradation in the quantitative metrics of signal and electrode quality: (signal-to-noise ratio, noise floor, peak amplitude, and neuronal yield). Implanted microelectrodes have been reported to suffer from time dependent degradation in signal quality due to tissue interface issues. Dealing with the experimental variability of chronically implantable arrays has been a formidable task because the sensor recording sites can be influenced by immune response, tissue encapsulation, and electrode structural changes to name a few [1]. These factors can cause the recording and impedance properties of the electrode to change over time. Therefore, the viability of chronic electrodes from single neurons has been limited to durations from a few months to a few years [2].

Two compelling perspectives for the effects that correlate with the observed degradation of the signal and electrode metrics in chronic neural recordings arise from the series of events that occurs after implantation. First, the BIOTIC observed effects include the inflammatory response, disruption of the blood–brain barrier (BBB), initiation of astrogliosis and recruitment of microglia and macrophages to the insertion site [3-6]. Second is the ABIOTIC observed effects, which includes the electrode physical changes (damaged insulation, change in surface area, oxidation/reaction, and corrosion) [7] that impact the electrical recording properties of the neural probe following prolonged exposure to brain extracellular fluids and molecules *in vivo*. Remarkably, each of these effects are typically studied independently even though understanding the true nature of the cause of electrode failure likely requires the coupling of both perspectives to obtain the complete picture. Current methods to assess electrode biocompatibility involve implanting a model electrode and studying the tissue response at various time points. However, biocompatibility being a functional characteristic requires analysis of tissue response in an electrically functional implant [1]. Moreover, existing studies lack quantitative and functional observations that directly link electrode recording properties (the detection of action potentials) to the mechanistic effects and possible predictors of failure. It is likely that this disconnect between the quantitative BIOTIC, ABIOTIC, and chronic FUNCTIONAL assessment has limited the success of approaches to understand the main factors that result in electrode degradation and of approaches to improve the electrode tissue interface [8, 9]. In this work, we create a new test bed that couples BIOTIC and ABIOTIC metrics to innovate how the mechanisms of electrode failure are measured and quantified.

Manuscript received April 15, 2011. This work was sponsored by the Defense Advanced Research Projects Agency (DARPA) Microsystems Technology Office under the auspices of Dr. Jack Judy (jack.judy@darpa.mil) through the Space and Naval Warfare Systems Center, Pacific Grant No. N66001-11-1-4009.

J. C..Sanchez and A. Prasad are with the Department of Biomedical Engineering and the Miami Project to Cure Paralysis, University of Miami, Coral Gables, FL 33146, USA (phone: 305-284-2330 e-mail: jcsanchez@miami.edu).

T. Nishida and V. Sankar are with the Department of Electrical and Computer Engineering, University of Florida, Gainesville, FL 32611, USA

J. R. Reynolds, A. L. Dyer, and E. Knott are with the Department of Chemistry, University of Florida, Gainesville, FL 32611, USA.

W. Streit, Q-S Xue, and G. Shaw are with the Department of Neuroscience, University of Florida, Gainesville, FL 32611, USA.

II. METHODS

Our experimental design is focused on a comprehensive temporal evaluation of biotic and abiotic metrics of primarily tungsten microwire electrode arrays implanted into the rat brain. It is known that within an implanted array not all electrodes fail at the same time and that there can be substantial variation in the lifetime of individual electrodes. Figure 1 shows a timeline of key phases known to be associated with electrode failure: Acute, Recovery, Chronic, and Failure. Thus, Fig. 1 is an average representation of identifiable phases useful for guiding our investigation.

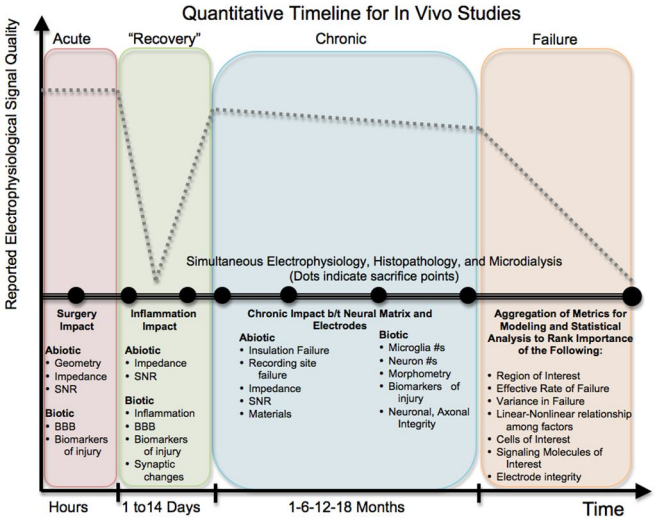

Figure 1. Coupling of biotic and abiotic metrics throughout electrode lifetime.

A. SEM Imaging

Scanning Electron Microscopic (CarryScope SEM, JEOL USA, Inc.) images of the tungsten microwire array were taken both pre- and post- implantation at 10KV accelerating voltage to evaluate the structural changes in the recording surface and the insulation of the wires. No conductive coating was used on the electrode sample. The post-implant images were taken after histological analysis was performed on the extracted electrode arrays.

B. Electrophysiology

A 16 channel microwire array was implanted in two adult male Sprague-Dawley rats. The array (TDT, FL) consisted of 50µm tungsten wires arranged in a 2x8 configuration. All animal procedures were approved by the University of Miami IACUC. A mid sagittal incision was made between the eyes to expose the top of the skull, and the landmarks bregma and lambda were identified on the skull. A craniotomy was drilled (-1mm posterior to bregma, 2.5mm lateral) at the site corresponding to somatosensory cortex. The electrode assembly was lowered using a micropositioner after removing the dura. While driving the electrode, electrophysiologic recordings were used to locate layer V pyramidal neurons (~1.6 mm from the cortical surface) where unit cell activity was found to be greatest. Once the array was positioned, it was supported with cranioplastic cement (Plastics-1) attached to a screw. The array was grounded using a second anchoring screw.

C. Recording Procedure and Data Analysis

Electrode impedance spectroscopy (nanoZ, TDT, FL) was performed before implantation and after each recording session. Fig. 2 shows the impedance spectroscopy plot for an array prior to implantation. Neuronal recordings obtained from the rats were processed and stored using a TDT RZ2 Real-time Signal Processing System (TDT, FL) sampling at 24414.06 Hz to record neuronal potentials from the microelectrode array. The neuronal potentials were band-pass filtered (0.3-6 kHz) and spike sorting [10] was performed to isolate single neurons in the vicinity of each electrode. All the microwires in Fig. 2 have a low impedance approximately between 10-100KΩ in the band-pass filtering range (0.3-6 kHz) suggesting the suitability of tungsten microwires for recording extracellular activity in the cortex. The array in the animal reported here was implanted for 18 days and neuronal signals were measured once a day on the following days post-surgery: 4, 5, 6, 7, 8, 11, 13, 15, 16, 17, and 18. The functional properties of the measured neuronal activity were quantified by the array yield, neuronal yield, and signal-to-noise ratio on each day of recording. In these experiments, the array yield represents the fraction of electrodes that produced at least a single neuron with discriminable action potentials. In neuroprosthetic applications, larger array yields are desirable because they correspond to arrays with more functional electrodes. The neuronal yield is calculated on a per-electrode basis and represents the number of discriminable neurons acquired from each electrode. Finally, the signal-to-noise ratio (SNR) indicates the usable dynamic range of the electrode to discern actual neural action potential signal from random background fluctuations. The SNR was calculated as the peak-to-peak voltage of the action potential divided by the RMS noise floor value. The noise floor was calculated as the RMS value of the signal for the duration of the maximum interspike interval.

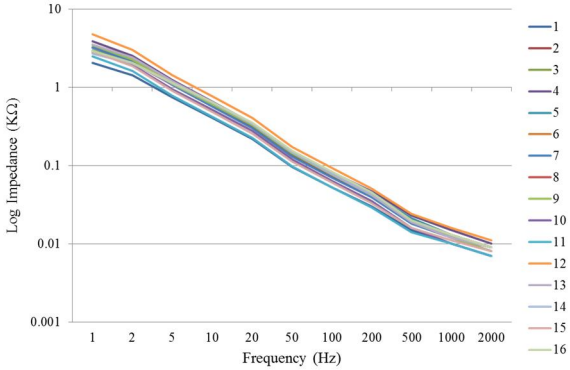

Figure 2. Pre-implant impedance spectroscopy for an array.

D. Cerebrospinal Fluid Sampling and Analysis

Cerebrospinal fluid (CSF) was acquired via puncture of the 4th ventricle (cisterna magna) [11]. CSF withdrawal was performed once a week and just prior to euthanasia on 3 rats, two implanted and one control (naïve). CSF from the control rat and the animal reported here (20µl) was run in duplicate wells on ELISA assays for pNF-H, UCHL1 and α-synuclein using procedures outlined in detail elsewhere [12-14].

E. Histology

The animals were transcardially perfused with a fixative solution containing 4% paraformaldehyde in 0.1 M phosphate-buffered saline (PBS; pH 7.4), the brain was removed, and electrodes gently removed from the brain. Prior to cryosectioning, tissues were cryoprotected using 30% sucrose in PBS and embedded with tissue freezing medium (TBS, #H-TFM). Frozen sections (20 m) were cut on a cryostat.

Double fluorescent immunolabeling was used for revealing the ED1 expression in the brain and its relation to microglial cells. ED1 was detected by a mouse anti-rat monocytes/macrophages CD68 monoclonal antibody (Chemicon; MAB1435; used at a dilution of 1:300) and microglia labeled by a polyclonal microglial marker, rabbit anti-Iba1, directed against the ionized calcium binding adaptor molecule 1 (Wako, 019-19741; diluted at 1:500). Sections were blocked with blocking buffer and incubated with the primary antibody. A combination of primary antibodies was applied to sections as cocktail primary antibodies. Cocktail secondary antibodies were then used for visualizing binding sites of primary antibodies. ED1 was visualized by goat anti-mouse IgG conjugated with Alexa Fluor 488 (Molecular probes, A11001; Eugene, OR; used at a dilution of 1:400), while Iba1 visualized by goat anti-rabbit IgG conjugated with Alexa Fluor 568 (Molecular probes, A11011; diluted at 1:400). Slides were examined with a Zeiss Axioskop 2 microscope. Digital images were captured with a Spot Slider 3 digital camera (Diagnostic Instruments Inc.; Sterling Heights, MI).

III. Results

A. Pre- and Post- Implant Structural Changes

It was observed from the pre-implant SEM image (Fig. 3 (left)) that all the wires displayed larger surface area at the recording tip with respect to the shank. This overhanging configuration (with the shape of a muffin top) was perceived as a result of the cutting adapted by the manufacturer. The images taken after explanting the electrodes from the brain (Fig. 3 (right)) did not show the presence of the overhanging configuration at the recording site. In addition, some wires showed deterioration of tungsten surface at the tips. These morphological changes indicate that the tungsten surface is subjected to corrosion during the implanted duration. However, corrosion rate seems to differ between wires, the reason for which is unclear at this stage. There aslo appears to be variations in the polyimide insulation.

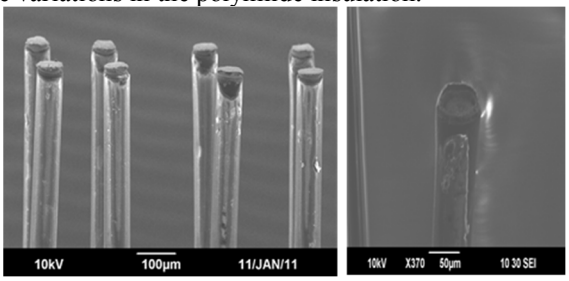

Figure 3. SEM images indicating abiotic morphological changes to the recording site and insulation. Pre-implant (left), Post-implant (right)

B. Time-Varying Functional Changes

Since chronic, microelectrode recording technologies are targeting single unit neuronal activity, we used the action potential as our standard for evaluation of data collected from the microelectrodes [15]. The 18-day implant functional performance presented here from R1 corresponds to the "recovery" period presented in Fig. 1. During this period, there have been anecdotal reports of variation both in the quality and number of discriminable neurons. Here we show with daily time resolution a quantification of the variance. In Fig. 4 (left), we show the percent neuronal yield from the entire array as a function of time. Initially, we observed a "blackout" period where few to no neurons could be discriminated across the electrode. In days 6-8 there was a step jump in activity across the array. However, this activity decreased on day 11 after which we observed a ramp increase in the yield over time. In Fig. 4 (right), the number of discriminable neurons on each electrode appeared to be spatially distributed with the largest neuronal yield on channels 1-8, however, the variance was similar across the array. In general, the noise floor values remained fairly constant with average values between 6-7µV for all electrodes. During the "recovery" period a general trend of an increase in SNR was observed on several but not all electrodes in the array. In Fig. 5, the increasing trend can be most clearly seen on channels 1-2 and 7-11. Other electrodes exhibited a heterogeneous relationship in SNR over time.

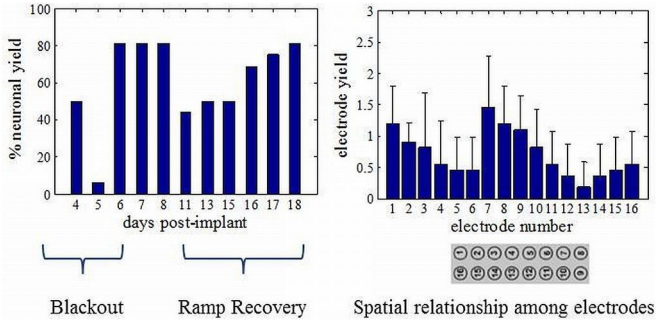

Figure 4. Temporal variation in electrode and neuronal yield.

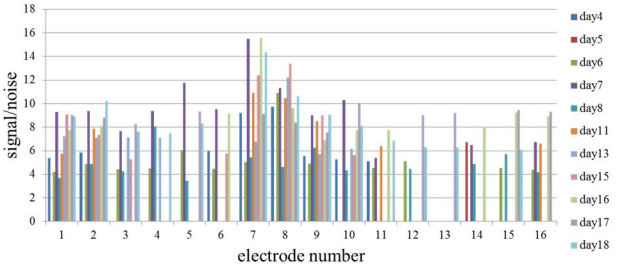

Figure 5. Temporal variation in SNR.

C. Microglia Activation

Increased microglia activation is observed in implanted tissue compared to the control. Figure 6 shows double immunofluorescent staining with Iba1 and ED1 antibodies to localize microglia and macrophages, respectively. Here, Panel A is the control side (left) and Panel B is the

implanted side (right). Sampling sites are shown in the inset diagram on Panel A. Note strong increase in ED1 (green) labeling around implantation tracks (B) indicating macrophage accumulation around electrodes. Numbers of microglia are greatly increased in B relative to A.

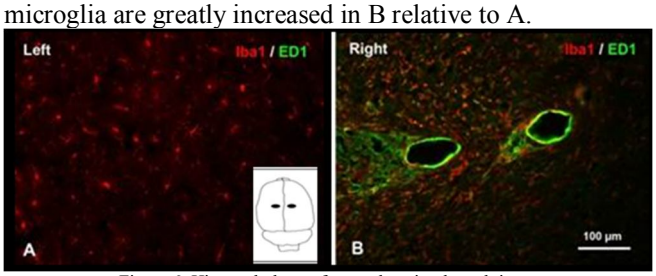

Figure 6. Histopathology of control vs. implanted tissue.

D. *Markers of Brain Injury*

Data for the pNF-H assay is shown in Fig. 7 below. Both the control and experimental animal showed signals, which were very close to background of the assay, and much below the signals obtained from human CSF samples ran on the same assay plates at the same time (the first 6 data points in Fig. 7). Similar results were obtained with UCHL1 and α-synuclein assays (not shown). We would expect to see no appreciable pNF-H, UCHL1 and α-synuclein signal in control CSF, as these proteins are only detected in significant amounts following CNS tissue loss. We conclude that the absence of signal in the experimental samples indicate that there was no appreciable CNS tissue loss as a result of the surgery in R1.

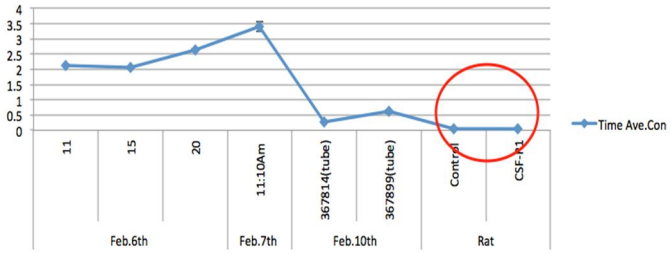

Figure 7. pNF-H level in CSF (Conc.ng/ml)

IV. Conclusions

The scientific perspective upon which we have based our work implies that, with a combined biotic and abiotic functional perspective, one may be able to explain underlying mechanisms governing the effects of chronic electrode implantation, as well as derive from the quantification predictions that would improve electrode performance in the future. As shown here, the results from each approach when considered together can provide a more complete understanding of the effects of the biotic-abiotic interactions [16]. To enable this study, we have developed a new testbed to investigate the spatiotemporal responses that occur at the most fundamental levels. This includes a combination of biotic and abiotic data acquisition that best captures the biochemical, structural, and electrophysiological responses in real-time. Toward this end, the composite, time-course, and resolution of Figures 3-7 provide some hints on the mechanisms of electrode performance and failure. For example, the initial "blackout" could be due to surgical tissue injury, while the ramp attributed to electrode electrical changes and microglial responses. However, to fully conclude on the acute, recovery, chronic and failure phases detailed Fig. 1, a more extensive study is required and is now underway in our laboratories.

References

[1] V. S. Polikov, P. A. Tresco, and W. M. Reichert, "Response of brain tissue to chronically implanted neural electrodes," *J Neurosci Methods,* vol. 148, pp. 1-18, Oct 15 2005.

[2] J. C. Williams, R. L. Rennaker, and D. R. Kipke, "Long-term neural recording characteristics of wire microelectrode arrays implanted in cerebral cortex," *Brain Research Protocols,* vol. 4, p. 303, 1999.

[3] L. Spataro, J. Dilgen, S. Retterer, A. J. Spence, M. Isaacson, J. N. Turner, and W. Shain, "Dexamethasone treatment reduces astroglia responses to inserted neuroprosthetic devices in rat neocortex," *Experimental Neurology,* vol. 194, p. 289, 2005.

[4] D. H. Szarowski, M. D. Andersen, S. Retterer, A. J. Spence, M. Isaacson, H. G. Craighead, J. N. Turner, and W. Shain, "Brain responses to micro-machined silicon devices," *Brain Research,* vol. 983, p. 23, 2003.

[5] L. Kam, W. Shain, J. N. Turner, and R. Bizios, "Correlation of astroglial cell function on micro-patterned surfaces with specific geometric parameters," *Biomaterials,* vol. 20, p. 2343, 1999.

[6] J. N. Turner, W. Shain, D. H. Szarowski, M. Andersen, S. Martins, M. Isaacson, and H. Craighead, "Cerebral Astrocyte Response to Micromachined Silicon Implants," *Experimental Neurology,* vol. 156, p. 33, 1999.

[7] L. A. Geddes and R. Roeder, "Criteria for the Selection of Materials for Implanted Electrodes," *Annals of Biomedical Engineering,* vol. 31, pp. 879-890, 2003.

[8] K. A. Moxon, S. C. Leiser, G. A. Gerhardt, K. A. Barbee, and J. K. Chapin, "Ceramic-Based Multisite Electrode Arrays for Chronic Single-Neuron Recording," *IEEE Trans. Biomedical Engineering,* vol. 51, pp. pp. 647-656, 2004 2004.

[9] J. K. Chapin and K. A. Moxon, Eds., *Neural Prostheses for Restoration of Sensory and Motor Function* (Methods and New Frontiers in Neuroscience. Boca Raton: CRC Press, 2001.

[10] M. S. Lewicki, "A review of methods for spike sorting: the detection and classification of neural action potentials," *Network: Computation in Neural Systems,* vol. 9, pp. R53-78, 1998.

[11] C. C. Pegg, C. He, A. R. Stroink, K. A. Kattner, and C. X. Wang, "Technique for collection of cerebrospinal fluid from the cisterna magna in rat," *Journal of Neuroscience Methods,* vol. 187, pp. 8-12, 2010.

[12] K. Boylan, C. Yang, J. Crook, K. Overstreet, M. Heckman, Y. Wang, D. Borchelt, and G. J. Shaw, "Immunoreactivity of the phosphorylated axonal neurofilament H subunit (pNF-H) in blood of ALS model rodents and ALS patients: Evaluation of blood pNF-H as a potential ALS biomarker " *Neurochem,* vol. 111, pp. 1182-1191, 2009.

[13] S. B. Lewis, W. R., L. Miralia, Y. Wang, C. Yang, and G. J. Shaw, "Identification and preliminary characterization of Ubiquitin C terminal Hydrolase 1 (UCHL1) as a biomarker of neuronal loss in aneurysmal subarachnoid hemorrhage," *J. Neurosci. Res.,* vol. 88, pp. 1475-1484, 2010.

[14] R. B. Tinsley, K. Kotschet, D. Modesto, H. Ng, Y. Wang, P. Nagley, G. Shaw, and M. K. Horne, "ELISA for detection of α-synuclein in human plasma," *J. Neurosci. Res.,* vol. 88, pp. 2693-2700, 2010.

[15] M. A. L. Nicolelis, *Methods for Neural Ensemble Recordings*. Boca Raton: CRC Press, 1999.

[16] T. W. Berger, J. K. Chapin, G. A. Gerhardt, D. J. McFarland, J. C. Principe, W. V. Soussou, D. M. Taylor, and P. A. Tresco, "WTEC Panel Report on International Assessment of Research and Development in Brain-Computer Interfaces," Baltimore, MD 2007.